sulphonate crosslinks further immobilizing the dopant polyions (evidenced by the emergence of S–O–C infrared vibrations[25] at 1,009 cm^{-1} and 833 cm^{-1}). Fabrication of 1.5 × 2.5 mm or 2.0 × 7.5 mm diodes was subsequently completed in the glove box without exposing to air. Calcium cathodes were evaporated at a base pressure < 10^{-6} mbar.

Characterization

IVL characteristics were collected on encapsulated devices or under vacuum using digital multimeters and a calibrated Si photodiode. Ionization potentials were estimated from the onset of the oxidation peak in cyclic voltammetry experiments. X-ray photoelectron spectroscopy was performed on a VG-220i-XL system with Al Kα X-rays. Spectroscopic ellipsometry was recorded on a UVISEL phase-modulated ellipsometer in the polarizer–compensator–sample–analyser configuration with 56.8° incidence angle. Atomic force microscopy was conducted on a Dimension 3100 microscope. Contact angle measurements were measured by a Krauss G20 drop shape analyser. Electroabsorption spectroscopy was performed on ITO/interlayer/green-emitting-PPV/Ca/Ag diodes.

Received 11 November 1999; accepted 1 February 2000.

1. Cao, Y., Parker, I. D., Yu, G., Zhang, C. & Heeger, A. J. Improved quantum efficiency for electoluminescence in semiconducting polymers. *Nature* **397,** 414–417 (1999).
2. Friend, R. H. *et al.* Electroluminescence in conjugated polymers. *Nature* **397,** 121–128 (1999).
3. Karg, S., Scott, J. C., Salem, J. R. & Angelopoulos, M. Increased brightness and lifetime of polymer light-emitting diodes with polyaniline anodes. *Synth. Met.* **80,** 111–117 (1996).
4. Carter, J. C. *et al.* Operating stability of light-emitting polymer diodes based on poly(p-phenylene vinylene). *Appl. Phys. Lett.* **71,** 34–36 (1997).
5. Decher, G. Fuzzy nanoassemblies: toward layered polymeric multicomposites. *Science* **277,** 1232–1237 (1997).
6. Onitsuka, O., Fou, A. C., Ferreira, M., Hsieh, B. R. & Rubner, M. F. Enhancement of light emitting diodes based on self-assembled heterostructures of poly(p-phenylene vinylene). *J. Appl. Phys.* **80,** 4067–4071 (1996).
7. Ho, P. K. H., Granström, M., Friend, R. H. & Greenham, N. C. Ultrathin self-assembled layers at the ITO interface to control charge injection and electroluminescence efficiency in polymer light-emitting diodes. *Adv. Mater.* **10,** 769–774 (1998).
8. Tai, K., Yang, L., Wang, Y. H., Wynn, J. D. & Cho, A. Y. Drastic reduction of series resistance in doped semiconductor distributed Bragg reflectors for surface-emitting lasers. *Appl. Phys. Lett.* **56,** 2496–2498 (1990).
9. Arkhipov, V. I., Emelianova, E. V., Tak, Y. H. & Bässler, H. Charge injection into light-emitting diodes: theory and experiment. *J. Appl. Phys.* **84,** 848–856 (1998).
10. Yoo, D., Shiratori, S. S. & Rubner, M. F. Controlling bilayer composition and surface wettability of sequentially adsorbed multilayers of weak polyelectrolytes. *Macromolecules* **31,** 4309–4318 (1998).
11. Lösche, M., Schmitt, J., Decher, G., Bouwman, W. G. & Kjaer, K. Detailed structure of molecularly thin polyelectrolyte multilayer films on solid substrates as revealed by neutron reflectometry. *Macromolecules* **31,** 8893–8906 (1998).
12. Dietrich, M., Heinze, J., Heywang, G. & Jonas, F. Electrochemical and spectroscopic characterisation of polyalkylenedioxythiophenes. *J. Electroanal. Chem.* **369,** 87–92 (1994).
13. Lögdlund, M., Lazzaroni, R., Stafström, S., Salaneck, W. R. & Brédas, J.-L. Direct observation of charge-induced pi-electronic structural changes in a conjugated polymer. *Phys. Rev. Lett.* **63,** 1841–1844 (1989).
14. Xing, K. Z., Fahlman, M., Chen, X. W., Inganäs, O. & Salaneck, W. R. The electronic structure of poly(3,4-ethylenedioxythiophene) studied by xps and ups. *Synth. Met.* **89,** 161–165 (1997).
15. van Slyke, S. A., Chen, C. H. & Tang, C. W. Organic electroluminescent devices with improved stability. *Appl. Phys. Lett.* **69,** 2160–2162 (1996).
16. Kim, J. S., Friend, R. H. & Cacialli, F. Surface energy and polarity of treated indium-tin-oxide anodes for polymer light-emitting diodes studied by contact-angle measurements. *J. Appl. Phys.* **86,** 2774–2778 (1999).
17. Campbell, I. H., Hagler, T. W. & Smith, D. L. Direct measurement of conjugated polymer electronic excitation energies using metal/polymer/metal structures. *Phys. Rev. Lett.* **76,** 1900–1903 (1996).
18. Brown, T. M. *et al.* Built-in field electroabsorption spectroscopy of polymer light-emitting diodes incorporating a doped poly(3,4-ethylenedioxythiophene) hole injection layer. *Appl. Phys. Lett.* **75,** 1679–1681 (1999).
19. He, Y., Gong, S., Hattori, R. & Kanicki, J. High performance organic polymer light-emitting heterostructure devices. *Appl. Phys. Lett.* **74,** 2265–2267 (1999).
20. Spreitzer, H. *et al.* Soluble phenyl-substituted PPVs - new materials for highly efficient polymer LEDs. *Adv. Mater.* **10,** 1340–1343 (1998).
21. Hung, L. S., Tang, C. W. & Mason, M. G. Enhanced electron injection in organic electroluminescence devices using an Al/LiF electrode. *Appl. Phys. Lett.* **70,** 152–154 (1997).
22. Kim, J. S., Ho, P. K. H., Greenham, N. C. & Friend, R. H. Electroluminescence emission pattern of organic light-emitting diodes: implications for device efficiency calculations. *J. Appl. Phys.* (in the press).
23. Harrison, N. T., Hayes, G. R., Phillips, R. T., & Friend, R. H. Singlet intrachain exciton generation and decay in poly(p-phenylenevinylene). *Phys. Rev. Lett.* **77,** 1881–1884 (1996).
24. Baldo, M. A., O'Brien, D. F., Thompson, M. E. & Forrest, S. R. Excitonic singlet-triplet ratio in a semiconducting organic thin film. *Phys. Rev. B* **60,** 14422–14428 (1999).
25. Colthup, N. B., Daly, L. H. & Wiberley, S. E. *Introduction to Infrared and Raman Spectroscopy* (Academic, New York, 1964).

Acknowledgements

We thank I. Grizzi, D. J. Lacey and E. P. Woo for support; J.-W. Cai for X-ray photoelectron spectroscopy; and A. Gerhard for electroabsorption measurements. P.K.H.H. is on leave from the National University of Singapore and thanks St John's College and IMRE for funding. This work was supported in part by the Engineering and Physical Sciences Research Council.

Correspondence and requests for materials should be addressed to R.H.F. (e-mail: rhf10@cam.ac.uk).

Effect of climate change relative to ozone depletion on UV exposure in subarctic lakes

Reinhard Pienitz & Warwick F. Vincent

Centre d'Études Nordiques, Université Laval, Québec, Canada G1K 7P4

The effect of stratospheric ozone depletion on increases in ambient levels of solar ultraviolet (UV) radiation in high-latitude regions[1] has raised concerns about the response of northern ecosystems to environmental change. The concentration of coloured dissolved organic material, which is derived from terrestrial vegetation and acts as a screen for ultraviolet radiation, is low in high-latitude lakes[2]. The underwater light environment in these lakes is therefore likely to be sensitive to small variations in the supply of this material, in addition to the effects of ozone depletion[2–5]. Here we use fossil diatom assemblages in combination with bio-optical models to estimate the magnitude of past variations in the underwater light regime of a lake at the boreal tree line. We find large shifts in underwater UV-B, UV-A and photosynthetically available radiation associated with changes in the input of coloured dissolved organic material into subarctic lakes during the Holocene. The inferred changes in biological exposure to UV radiation were at least two orders of magnitude greater than those associated with moderate (30%) ozone depletion. Our findings indicate that freshwater ecosystems at present located across vegetation gradients will experience significant shifts in underwater spectral irradiance through the effects of climate change on catchment vegetation and the export of coloured dissolved organic material.

To address the potential effect of climate change relative to ozone depletion on northern freshwater ecosystems, we combined palaeolimnological analyses with bio-optical models based on present-day conditions. Specifically, we estimated past underwater light conditions from concentrations of dissolved organic carbon (DOC, a correlate of coloured dissolved organic material, CDOM[2–5]) that were inferred from fossil diatom assemblages preserved in Holocene sedimentary deposits[6]. Strong statistical relationships exist between diatom community structure and organic carbon concentrations[7–9], which have been used to infer past DOC concentrations from fossil diatom records[6,10]. The sediments were sampled from Queen's Lake (unofficial name; latitude 64°07′N, longitude 110°34′W; Fig. 1) in the central Northwest Territories, Canada. The lake basin is located on Precambrian granites of the Canadian Shield ~25 km north of the mapped limit of the central Canadian tree line, and lies on the boundary between the high subarctic and low Arctic ecoclimate

Table 1 Inferred DOC changes in two subarctic lakes during the Holocene

Period	Dates	Queen's Lake		Toronto Lake
	(kyr BP)	DOC (mg l^{-1})	DV (10^7 g^{-1})	DOC (mg l^{-1})
Post	<3	1.4 (0.2)	5.33 (1.5)	2.8 (0.2)
Mid	3–5	5.6 (0.2)	21.09 (3.3)	4.2 (0.1)
Pre	>5	1.8 (0.3)	8.87 (2.1)	n.d.

Each value is the mean (± s.e.) for the period after (Post), during (Mid) and before (Pre) the mid-Holocene warm interval for the central Canadian treeline region. A two-way ANOVA analysis (general linear model, unequal design, no interaction terms) of the DOC data for the two lakes showed that there are statistically significant effects of period ($F = 57.1$; $P < 0.001$) but no significant differences between lakes ($F = 1.3$; $P = 0.26$). A subsequent Tukey multiple comparison test showed a significant increase between Pre and Mid ($P < 0.001$), a significant decrease between Mid and Post ($P < 0.001$), but no significant difference between Pre and Post ($P = 0.112$) periods. Diatom valve concentrations were higher during the mid-Holocene warm interval ($P < 0.05$; Tukey multiple comparison test) relative to Pre and Post periods, which were not significantly different from each other ($P = 0.73$). DV, diatom valves; n.d., not determined because the diatom community composition was outside the bounds of the training set.

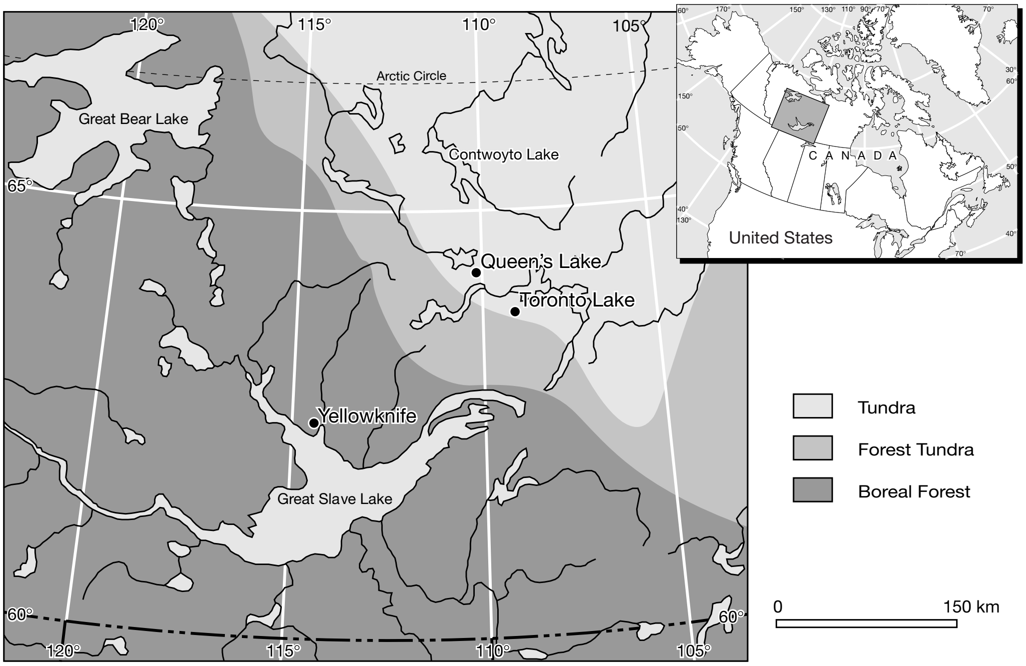

Figure 1 Location of study sites near the northern tree line in central Canada. The catchments of both lakes are typified by rolling terrain, composed mainly of Proterozoic intrusive granites (granodiorites). Cryic regosols and organic soils are found on discontinuous glacial overburden underlain by permafrost. Queen's Lake (480 m above sea level, a.s.l.; area, 50 ha; depth, 3.5 m) is a closed basin, whereas Toronto Lake (414 m a.s.l.; area, 10 ha; depth, 6.75 m) is hydrologically open and drains an extensive headwater catchment (~2,900 ha). Both lakes are located in *Betula glandulosa* tundra, with a few patches of *Picea mariana* Krummholz in sheltered locations. Further details on regional geology, climate and soils are given in refs. 11, 12, 14.

regions. The tree line is defined as the zone of transition between closed continuous forest and tundra. Details on diatom stratigraphies and sediment core chronology are presented and discussed elsewhere[6,11].

Diatom community structure and diatom-inferred DOC concentrations show three distinct and abrupt successional changes over the history of Queen's Lake (Fig. 2a, b). A major shift occurred between ~5 and ~3 kyr before present (BP) in the proportion of periphytic versus planktonic diatom species, corresponding to peak abundance (>70%) of periphytic taxa and a strong decline in the relative abundance of planktonic species. This period also corresponded to a significant increase in the total diatom population, as suggested by peak concentrations of diatom valves per unit sediment (Table 1); the shift towards periphyton dominance at this time was therefore not simply a result of reduced plankton concentrations. The profile of diatom-inferred DOC indicates highest levels between 5 and 3 kyr BP, showing a threefold increase in concentrations when compared with the periods preceding and following this mid-Holocene warm interval (Fig. 2c). The diatom-based reconstruction then indicates a sharp decline (~88%) in DOC concentrations over the most recent 3,000 years.

These biological and chemical shifts correspond with other evidence of major climatic and other environmental changes in central Canada following local deglaciation around 9 kyr BP; this period was characterized by the advance and subsequent retreat of the boreal tree line[11–13], accompanied by profound limnological and hydrological changes[6,11,14], in response to shifts in the mean summer position of the Arctic frontal zone[15]. Terrestrial vegetation abruptly shifted from dwarf shrub tundra to *Picea mariana* forest-tundra about 5 kyr BP, as the frontal zone moved northwards. Minor local fluctuations in treeline position or forest density occurred during the period of maximum forest cover (forest-tundra) between 5 and 3 kyr BP, followed by a return to the current dwarf shrub tundra vegetation after 3 kyr BP[11].

DOC concentration, and its correlates water colour and CDOM, decline abruptly with decreasing forest cover across the northern tree line[3,16,17]. As found for shifts in the alpine tree line[18], the Holocene vegetational changes in central Canada are likely to have been accompanied by significant variations in the export of CDOM (mostly humic and fulvic acids) from the catchments, which in turn would influence the underwater UV radiation in their receiving waters. Our data from Queen's Lake are consistent with such effects, and suggest that the highest sustained lakewater DOC concentrations coincided with the period of maximum tree-line advance and/or highest forest cover density during the mid-Holocene (about 5,000–3,000 years ago). These limnological changes are not unique to the Queen's Lake site, as similar diatom and DOC records have been obtained from another treeline lake (Toronto Lake, Fig. 1; Table 1)[6,11], reflecting the regional character of climatic, vegetational and limnological changes that occurred near the northern tree line in central subarctic Canada during the Holocene[12–14].

The large and rapid changes in DOC imply that Queen's Lake also experienced significant shifts in the underwater optical environment over the past 6,000 years, as its correlate CDOM is the main attenuator of UV radiation and photosynthetically available radiation (PAR) in oligotrophic lakes of northern regions, including the boreal forest[2,5]. Application of our bio-optical models (which have been derived from measurements in high-latitude waters, including lakes across the North American tree line) showed that the inferred DOC shifts were equivalent to a decrease by two orders of magnitude in biologically effective UV exposure between 6 kyr BP and the mid-Holocene vegetation maximum; the most recent 3,000 years would have been characterized by a >50-fold increase to present-day values (Fig. 2d).

These effects were consistently large for two different biological weighting functions; the first for DNA damage (particularly sensitive to UV-B) and the second for UV-photoinhibition of algal photosynthesis (sensitive to UV-A plus UV-B). The inferred DOC shifts also imply substantial changes in underwater PAR over the course of the Holocene, with minimum light availability for photosynthesis during the vegetation maximum. This PAR effect

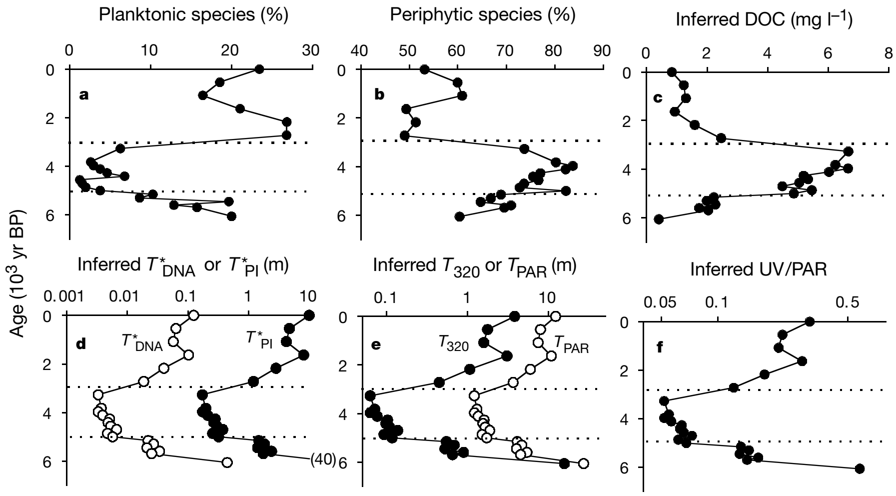

Figure 2 Changes in diatom community structure and inferred variables in Queen's Lake. The diatom data are expressed as the percentage of the total number of valves in each sample associated with planktonic or benthic taxa. Diatom species data were used to infer DOC (mg l^{-1}), biologically weighted UV exposure (T^*_{PI} or T^*_{DNA}) and underwater spectral balance (water column transparency for 320-nm UV radiation (T_{320}), PAR (T_{PAR}), and the ratio between the two (UV/PAR)) over the past 6,000 years. The dotted lines show the period of mid-Holocene maximum forest cover.

was less than for UV radiation (Fig. 2e), and the inferred water column ratio of UV radiation (at 320 nm) to PAR dropped by an order of magnitude between 6 to 3.5 kyr BP, followed by a >5-fold rise over the last 3,000 years (Fig. 2f). We note that the vegetation maximum also corresponds to the period of large increase in periphytic diatom taxa relative to planktonic diatoms. The planktonic species may have been more sensitive to PAR-limitation in the less transparent waters during this period of high DOC. Conversely, the periphyton may have been less UV-inhibited at this time, given the substantially reduced UV/PAR ratio. Elsewhere in Canada, UV radiation has been shown to have a pronounced impact on periphytic algal communities in shallow lakes[19], and decreased UV exposure in shallow littoral habitats may be one reason for the predominance of periphytic diatom taxa during periods of high DOC, lowest biologically effective UV exposure and lowest water transparency.

The biologically weighted UV transparency parameter (T^*, Fig. 2) allows a comparison of the effects of DOC change with those associated with stratospheric ozone depletion on a common, biologically relevant, scale. For this analysis we recomputed T^* for a 30% decline (over the period late 1970s to early 1990s there was a 10% depletion of ozone over the Arctic[1], with more recent evidence of up to 40% depletion in early spring[20]) in stratospheric ozone, from 330 to 230 Dobson units (DU). Under DOC conditions of 1 mg C l^{-1} (the approximate value inferred for Queen's Lake for the past 1,000 years), this would result in a 24% increase in biological UV exposure weighted for DNA effects, and a 0.9% increase weighted for photoinhibition effects. These increases are small relative to those calculated from the changes in inferred DOC over the past 6,000 years: from the vegetation maximum to the present, the estimate of T^* for DNA increases by 5,651% while T^* for photoinhibition increases by 3,658%. The latter is especially striking relative to the ozone effect. This is because, in contrast to ozone, CDOM controls UV-A as well as UV-B attenuation, and UV-A is a significant control on photoinhibition under natural spectral regimes[21].

Numerical integration of weighted UV radiation from the surface to the current maximum depth of the lake (3.5 m) confirmed the much greater effect of changes in dissolved colour. For the more ozone-sensitive DNA effect, this calculation gave a total water column weighted UV that was 118% higher under conditions of 230 DU but 1,079% higher under the inferred DOC reduction; the equivalent increases for UV-photoinhibition were 7% (reduced ozone) and 1,456% (reduced colour). We note, however, that the ozone depletion effect is taking place over a timescale of decades, while the vegetation-related changes are likely to have occurred over a timescale of 100 years and longer.

The T^* estimates based on DOC must be considered a lower bound to variability in underwater UV exposure; this exposure is also influenced by other variables, including biotic and abiotic particle concentrations, and climate-related changes in cloud, lake-ice and snow cover. Changes in lake depth and mixing regimes[3], as well as threshold, recovery and other nonlinear effects of UV exposure on biological processes, will also contribute to the variability in response. However, these calculations provide evidence for significant variations in biological UV exposure during the Holocene that far exceed those associated with current levels of ozone depletion, and they draw attention to the sensitivity of these freshwater ecosystems to future shifts in vegetation and hydrology associated with global climate change.

Global warming scenarios predict a seasonal or annual warming of the order of 1–4 °C in the treeline zone of Canada in the next century[22]. Examination of past warm episodes, such as the mid-Holocene climate optimum, may provide the best available analogue scenarios with respect to the anticipated climate warming and its associated limnological and hydrological effects. The potential for a large northward displacement of the forest boundary in central Canada[23] and the effect of such a displacement on climate[24] makes it important to understand the potential response of this region and its abundant freshwater ecosystems to climate change. It is likely that warming would lead to relatively rapid infilling of forest in the forest-tundra zone and associated changes in the physical and chemical conditions of freshwater lakes[6], with ecologically significant effects within ~100–150 years (refs 11, 13). The Holocene chemical and bio-optical changes inferred for Queen's Lake are likely to be representative of many lakes across the circumpolar treeline region, as well as other ecotonal boundaries such as the alpine tree line, and this study provides some insights into the likely response of freshwater aquatic ecosystems at the tree line to future warming.

The history of palaeo-optical conditions inferred from Queen's Lake implies that aquatic biota of lakes in the boreal treeline zone may have experienced their greatest UV exposure immediately following Holocene deglaciation (before the development of CDOM sources in the catchment) and during subsequent episodes of reduced CDOM inputs; such episodes occurred when climate cooling reduced forest canopy and shifted the tree line, ultimately causing the catchment basin to lose its forest cover (for example, the Neoglacial period of colder and drier climate conditions since ~3 kyr BP[6,14]). Our study also shows that global warming effects in lakes located near the present-day northern boundary of the boreal forest may be very different from those observed in Precambrian Shield lakes to the south, where some lakes lost 50% of their DOC over a 20-year period during the 1970s and 1980s due to acidification and climate warming[4,25]. UV penetration in dilute lakes that are presently within catchments dominated by tundra and forest-tundra may be significantly reduced whenever climate warming induces northward shifts of tree line or increases in the density of forest cover, leading to increased terrestrial CDOM inputs. The reduced UV-inhibition of biological processes is partially offset, however, by reduced underwater light for photosynthesis and decreased photochemical degradation of DOC into substrates that are more available for bacterial production. Also, changes in wetland patterns in the catchment associated with warmer conditions are likely to modify DOC concentrations in the recipient lakes[26]. Lakes with the highest catchment area to lake volume ratios are likely to be the most affected by these vegetational changes.

Our palaeo-optical analysis of Queen's Lake shows that the UV climate of lakes at, and near, the tree line may have been changed more radically by climate change than by moderate ozone depletion. The Holocene record provides a window into future changes in this vast circumpolar biome, and implies that current warming trends in the subarctic may lead to significant shifts in underwater spectral balance, PAR availability and UV radiation exposure for aquatic organisms. □

Methods

Palaeolimnological analysis

Queen's Lake and Toronto Lake were sampled in the region of maximum depth where the sediments provided an integration of material from the littoral zone (containing periphyton) as well as the offshore limnetic zone (containing phytoplankton). Sediment samples were taken at 2.5-cm intervals from the AMS ^{14}C-dated sediment cores; diatoms were extracted, isolated, identified and quantified following standard procedures[6,11].

Past DOC concentrations in Queen's Lake were reconstructed from the relative abundances of fossil diatoms using a weighted-averaging partial least squares (WA-PLS) transfer function for DOC developed from diatoms in dilute, oligotrophic lakes from the study region in the central Northwest Territories[6], and therefore appropriate for Queen's Lake. Development of the diatom-DOC model involved a two-step analytical approach[6]. First, responses of modern diatoms to DOC in a set of lakes equally distributed across the northern tree line (DOC gradient, 1.6–9.1 mg l^{-1}; $n = 22$) were modelled in a weighted-averaging (WA) regression. Second, these modelled responses were used to infer past DOC concentrations from the composition of fossil diatom assemblages using WA calibration. The root-mean-squared error of prediction in the estimates of inferred DOC is 1.3 mg C l^{-1} with a jack-knifed r^2 of 0.61 for the diatom-DOC model as calculated by WAPLS version 1.1 (S. Juggins and C.J.F. ter Braak). Performance measures (program ANALOG; J. M. Line and H. J. B. Birks) of the diatom inference model indicated that no-analogue situations with modern diatom communities did not occur in the Queen's Lake core, but within the period preceding the mid-Holocene warm interval in the Toronto Lake core[6]. Data for planktonic and periphytic diatoms and diatom-inferred DOC were based on a total of 76 taxa.

Biological UV exposure

Weighted transparency values (T^*) allowed the relative effects of UV attenuation in the atmosphere and water to be assessed on a common, biologically relevant scale[27]. T^* is defined as $\int 1/K(\lambda)\epsilon(\lambda)E_{0\mathrm{rel}}(\lambda)F(\lambda)\mathrm{d}\lambda$, where the integral is evaluated over the UV-B plus UV-A wavelength range (280–400 nm). $K(\lambda)$ is the diffuse attenuation coefficient at wavelength λ calculated from statistical relationships with DOC for high-latitude lakes[27]; $\epsilon(\lambda)$ is the biological weighting factor for DNA damage[28] (T_{DNA}) or for UV-photo-inhibition of photosynthesis[21] (T^*_{PI}) and set on a relative scale ($\epsilon = 1.0$ at 300 nm); $E_{0\mathrm{rel}}(\lambda)$ is the normalized surface irradiance at Churchill in subarctic Manitoba ($E_{0\mathrm{rel}} = 1.0$ at 400 nm; we used an incident UV radiation spectrum for Churchill (lat. 58° 75′ N, long. 94° 07′ W) at low zenith angle (36.57°) from the World Ozone and Ultraviolet Radiation Data Center database, World Meteorological Organization, Toronto); and $F(\lambda)$ is the factor of enhancement in surface radiation flux for a given stratospheric ozone depletion[29] (set to 1.0 for 330 DU). T^* values were calculated at 1-nm intervals and then summed from 290 to 400 nm to give a total T^* for UV radiation. T^* is analogous to other oceanographic indices based on transparency ($1/K$), such as critical depth and average water column irradiance.

Received 28 October 1999; accepted 16 February 2000.

1. International Arctic Science Committee *Effects of Increased Ultraviolet Radiation in the Arctic* (Report No. 2, IASC, Oslo, 1995).
2. Laurion, I., Vincent, W. F. & Lean, D. R. S. Underwater ultraviolet radiation: development of spectral models for northern high latitude lakes. *Photochem. Photobiol.* **65,** 107–114 (1997).
3. Vincent, W. F. & Pienitz, R. Sensitivity of high latitude freshwater ecosystems to global change: temperature and solar ultraviolet radiation. *Geosci. Can.* **23,** 231–236 (1996).
4. Schindler, D. W., Curtis, P. J., Parker, B. R. & Stainton, M. P. Consequences of climate warming and lake acidification for UV-B penetration in North American boreal lakes. *Nature* **379,** 705–708 (1996).
5. Williamson, C. E., Stemberger, R. S., Morris, D. P., Frost, T. M. & Paulsen, S. G. Ultraviolet radiation in North American lakes: Attenuation estimates from DOC measurements and implications for plankton communities. *Limnol. Oceanogr.* **41,** 1024–1034 (1996).
6. Pienitz, R., Smol, J. P. & MacDonald, G. M. Paleolimnological reconstruction of Holocene climatic trends from two boreal treeline lakes, Northwest Territories, Canada. *Arct. Antarct. Alp. Res.* **31,** 82–93 (1999).
7. Pienitz, R. & Smol, J. Diatom assemblages and their relationship to environmental variables in lakes from the boreal forest-tundra ecotone near Yellowknife, Northwest Territories, Canada. *Hydrobiologia* **269/270,** 391–404 (1993).
8. Battarbee, R. W., Flower, R. J., Juggins, S., Patrick, S. T. & Stevenson, A. C. The relationship between diatoms and surface water quality in the Høylandet area of Nord-Trøndelag, Norway. *Hydrobiologia* **348,** 69–80 (1997).
9. Fallu, M. -A. & Pienitz, R. Diatomées lacustres de Jamésie-Hudsonie (Québec) et modèle de reconstitution des concentrations de carbone organique dissous. *Écoscience* **6,** 603–620 (1999).
10. Korsman, T., Renberg, I. & Anderson, N. J. A palaeolimnological test of the influence of Norway spruce (*Picea abies*) immigration on lake-water acidity. *Holocene* **4,** 132–140 (1994).
11. MacDonald, G. M., Edwards, T. W. D., Moser, K. A., Pienitz, R. & Smol, J. P. Rapid response of treeline vegetation and lakes to past climate warming. *Nature* **361,** 243–246 (1993).
12. Moser, K. A. & MacDonald, G. M. Holocene vegetation change at treeline north of Yellowknife, Northwest Territories, Canada. *Quat. Res.* **34,** 227–239 (1990).
13. MacDonald, G. M., Szeicz, J. M., Claricoates, J. & Dale, K. A. Response of the central Canadian treeline to recent climatic changes. *Ann. Assoc. Am. Geogr.* **88,** 183–208 (1998).
14. Wolfe, B. B., Edwards, T. W. D., Aravena, R. & MacDonald, G. M. Rapid Holocene hydrologic change along boreal treeline revealed by $\delta^{13}C$ and $\delta^{18}O$ in organic lake sediments, Northwest Territories, Canada. *J. Paleolimnol.* **15,** 171–181 (1996).
15. Pielke, R. A. & Vidale, P. L. The boreal forest and the polar front. *J. Geophys. Res.* **100,** 25755–25758 (1995).
16. Engstrom, D. R. Influence of vegetation and hydrology on the humus budgets of Labrador lakes. *Can. J. Fish. Aquat. Sci.* **44,** 1306–1314 (1987).
17. Pienitz, R., Smol, J. P. & Lean, D. R. S. Physical and chemical limnology of 24 lakes located between Yellowknife and Contwoyto Lake, Northwest Territories (Canada). *Can. J. Fish. Aquat. Sci.* **54,** 347–358 (1997).
18. Leavitt, P. R., Vinebrooke, R. D., Donald, D. B., Smol, J. P. & Schindler, D. W. Past ultraviolet radiation environments in lakes derived from fossil pigments. *Nature* **388,** 457–459 (1997).
19. Vinebrooke, R. D. & Leavitt, P. R. Effects of ultraviolet radiation on periphyton in an alpine lake. *Limnol. Oceanogr.* **41,** 1035–1040 (1996).
20. Hansen, G. & Chipperfield. M. P. Ozone depletion at the edge of the Arctic polar vortex 1996/1997. *J. Geophys. Res.* **104,** D1, 1837–1845 (1998).
21. Cullen, J. J., Neale, P. J. & Lesser, M. P. Biological weighting function for the inhibition of phytoplankton photosynthesis by ultraviolet radiation. *Science* **258,** 646–650 (1992).
22. Houghton, J. T. *et al.* (eds) *Climate Change 1995: The Science of Climate Change* (Cambridge Univ. Press, Cambridge, 1996).
23. Smith, T. M., Shugart, H. H., Bonan, G. B. & Smith, J. B. Modeling the potential response of vegetation to global climate change. *Adv. Ecol. Res.* **22,** 93–116 (1992).
24. Foley, J. A., Kutzbach, J. E., Coe, M. T. & Levis, S. Feedbacks between climate and boreal forests during the Holocene epoch. *Nature* **371,** 52–54 (1994).
25. Yan, N. D., Keller, W., Scully, N. M., Lean, D. R. S. & Dillon, P. J. Increased UV-B penetration in a lake owing to drought-induced acidification. *Nature* **381,** 141–143 (1996).
26. Urban, N. R., Bayley, S. E. & Eisenreich, S. J. Export of dissolved organic carbon and acidity from peatlands. *Wat. Resour. Res.* **25,** 1619–1628 (1988).
27. Vincent, W. F., Laurion, I. & Pienitz, R. Arctic and Antarctic lakes as optical indicators of global change. *Ann. Glaciol.* **27,** 691–696 (1998).
28. Setlow, R. B. The wavelengths in sunlight effective in producing skin cancer: a theoretical analysis. *Proc. Natl. Acad. Sci. USA* **71,** 3363–3366 (1974).
29. Frederick, J. E. & Snell, H. E. Ultraviolet radiation levels during the Antarctic spring. *Science* **241,** 438–440 (1988).

Acknowledgements

We thank G. M. MacDonald for providing the sediment cores, and J. J. Cullen, J. A. E. Gibson, C. Lovejoy and D. W. Schindler for their comments on the manuscript. This work was supported by Fonds pour la Formation de Chercheurs et l'Aide à la Recherche (Québec), Natural Sciences and Engineering Research Council of Canada and Centre d'Études Nordiques.

Correspondence and requests for materials should be addressed to R.P. (e-mail: reinhard.pienitz@cen.ulaval.ca) or W.F.V. (e-mail: warwick.vincent@bio.ulaval.ca).